Scientific Research Publishing

Journal of Modern Physics, 2022, 13, 1331-1340
https://www.scirp.org/journal/jmp
ISSN Online: 2153-120X
ISSN Print: 2153-1196

Possible Neutrino-Antineutrino Production during Gamma Ray e−e+ Pair Production: Monte Carlo Simulation Study

Michael Bettan[1,2], Jonathan Walg[1], Itzhak Orion[1*]

[1]Department of Nuclear Engineering, Ben-Gurion University of the Negev, Beer-Sheva, Israel
[2]Soreq NRC, Yavne, Israel
Email: *iorion@bgu.ac.il

How to cite this paper: Bettan, M., Walg, J. and Orion, I. (2022) Possible Neutrino-Antineutrino Production during Gamma Ray e−e+ Pair Production: Monte Carlo Simulation Study. *Journal of Modern Physics*, **13**, 1331-1340.
https://doi.org/10.4236/jmp.2022.1311082

Received: October 6, 2022
Accepted: November 1, 2022
Published: November 4, 2022

Abstract

An alternative Feynman diagram for electron-positron pair production, in which neutrino and antineutrino are also produced on the same pathway, is introduced here. In the proposed pair production process, a portion of the momentum is carried by neutrinos and antineutrinos, allowing the rest of the momentum for the electron-positron pair. Simulations to inspect the proposed pair production process were conducted in this research using the EGS5 code system while modifying its subroutine "PAIR". Liquid Xenon detector was then positioned in the path of various mono-energetic photon beams ranging from 2.6 to 12 MeV. These simulations were intended to inspect the detectability of the alternative pair production effects on radiation measurements in order to assess the detection conditions. Simulation results provided a comparison between the original pair production process and the proposed pair production process. Spectral results showed that changes in the region around 1 - 2 MeV and in the photopeak region were remarkable, therefore detectable. Further experimental research is recommended based on simulation findings. The alternative pair production process, firstly introduced in this paper, led to production of a larger flux of neutrinos from gamma radiation. This additional neutrino production and its contribution to non-baryonic dark matter are discussed.

Keywords

Gamma, Pair-Production, Radiation, Neutrino, Dark-Matter

1. Introduction

1.1. The Neutrino Emission Prediction

When beta decay was first discovered, the process showed a continuous spec-

trum of the emitted electron from the nucleus. This continuous spectrum meant that some of the emitted electrons carry only part of the energy. Since energy must be conserved, the question arose: what happened to the missing energy? This continuous spectrum led to the assumption by Pauly of a new, small elementary particle emitted in the beta decay, the Neutrino [1]. The theoretically predicted Neutrino, a half-spin, zero-electric charge, and low mass elementary particle which carries energy and momentum interacts with the nuclear fields [2]. Later, the beta emission probabilities were formulated by the Fermi golden rules for beta decay.

1.2. Matter and Anti-Matter

In the wake of quantum theory development, P. Dirac established an equation to introduce relativistic Hamiltonian that includes the spin-1/2 property of particles. Solutions for this Dirac equation predicted that each elementary particle should have an anti-matter companion. Anti-matter particle has the same mass, an opposite electric charge, and opposite magnetic moment direction [3]. Hence, the counterpart of an electron is a positron. C. D. Anderson first detected in 1932 the anti-electron in cosmic rays, subsequently confirming the Dirac prediction of existence of anti-matter [4].

1.3. Rules for e−e+ Production

Photons transported through matter have the probability to produce pairs of matter-antimatter, such as e−e+, if two conditions are fulfilled: 1) photon energy is above a threshold dictated by the rest mass of the pair of particles, and 2) the presence of an electromagnetic field within the photon path. Thus, pair production cross section is linearly dependent on the atomic Z-number for atomic electron field interactions, as well as dependent on the square of Z for nuclear field interactions [5]. The theory of photon bound-free pair production has been gradually developed since the 1930s, while calculations of e−e+ cross sections for a vast range of photon energies and for various materials began accumulating during the 1960s. Full historical progress and references for the development of pair production theory and calculations are presented in detail in Reference [6]. Recently more detailed cross-section dependence on the target nucleus's magnetic field compared to the nucleus's electric field was investigated [7]. Several Monte Carlo code systems have been implemented for photon transport at energies of 1 keV up to 100 GeV after accomplishing numerical cross sections for photon interactions, including pair production. The most well-known Monte Carlo code system is the MCNP; first released in 1977, this initial version did not include the electron transport process [8]. Released in 1982 the MC tool kit GEANT-3 enabled full photon-electron transport; after 2000, this version was replaced by the upgraded GEANT4 code system [9]. EGS (Electron Gamma Shower) is one of the leading code systems for simulating high-energy gamma ray interactions in matter. Although the EGS3 version released in 1978 was designed to simulate

electromagnetic cascade for high physics experiments, simulation of pair production that can take place only by gammas with energies above 1.02 MeV and that becomes significant at energies above 2.5 MeV, was first introduced in the conversion of EGS3 to EGS4 in 1985 [10]. Each of these code systems was gradually upgraded, mostly by modifying cross section libraries. Approximately twenty years later, a tremendous change was made to every code that included modifications in transport handling.

1.4. Neutrino as a Dark Matter (Puzzle)

Dark matter is a cosmological term that expresses missing mass in the Universe due to the observed large-scale expansion rate, or the Hubble constant [11]. Current gravitational modeling indicates that whereas a great amount of the mass in the Universe influences Universe dynamics, it is not detectable by common observational methods [12]. Several theoretical proposals based on the Standard Model (SM) of particle physics (or beyond SM) explain this dark matter phenomenon; in these proposals hidden non-baryonic particle content is presumed. A review paper by G. Bertone, D. Hooper, and J. Silk introduces the particle dark matter candidates' properties and their detectability [13]. SM particle as the neutrino (or antineutrino) is likely to be a candidate for non-baryonic dark matter because of its low interaction probability due to its sub-electron Volt rest-mass [14], as well as its neutral electric charge, and minuscule absorption cross section. A detailed discussion by Kreisch *et al.* regarding neutrinos as dark matter was later published as "Neutrino puzzle: Anomalies, interactions, and cosmological tensions". In Reference [15], the known processes that produce neutrino flux in the galaxy are estimated to contribute a mass which is too small compared to the estimated total dark matter density [16]. This estimation of neutrino contribution to dark matter might be altered with the development of more highly efficient neutrino telescopes, or by discovering new neutrino emission processes.

2. Methods

In **Figure 1**, the Feynman diagram for pair production (PP) is shown. In this study we introduce an alternative Feynman diagram for pair production in which neutrinos and antineutrinos are also produced via the same pathway (**Figure 2(a)** and **Figure 2(b)**). In this case, neutrinos and antineutrinos should escape with a certain amount of the total momentum and energy, while conserving momentum and energy. Accordingly, we prepared a setup to simulate and track the response to this proposed change in the pair production process via the electron and positron contribution to an Xe detector. Liquid Xe detectors are state-of-the-art scintillation systems for radiation and particle tracking that could suit the PP interaction detection outcome [17] [18].

Significant improvements to the pair production subroutine that could better simulate the process using higher energy gamma rays were introduced only in

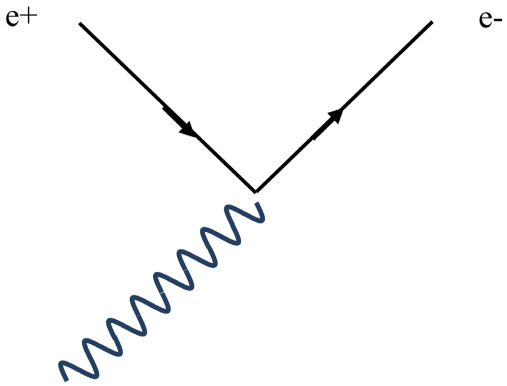

Figure 1. Feynman diagram of electron-positron pair production.

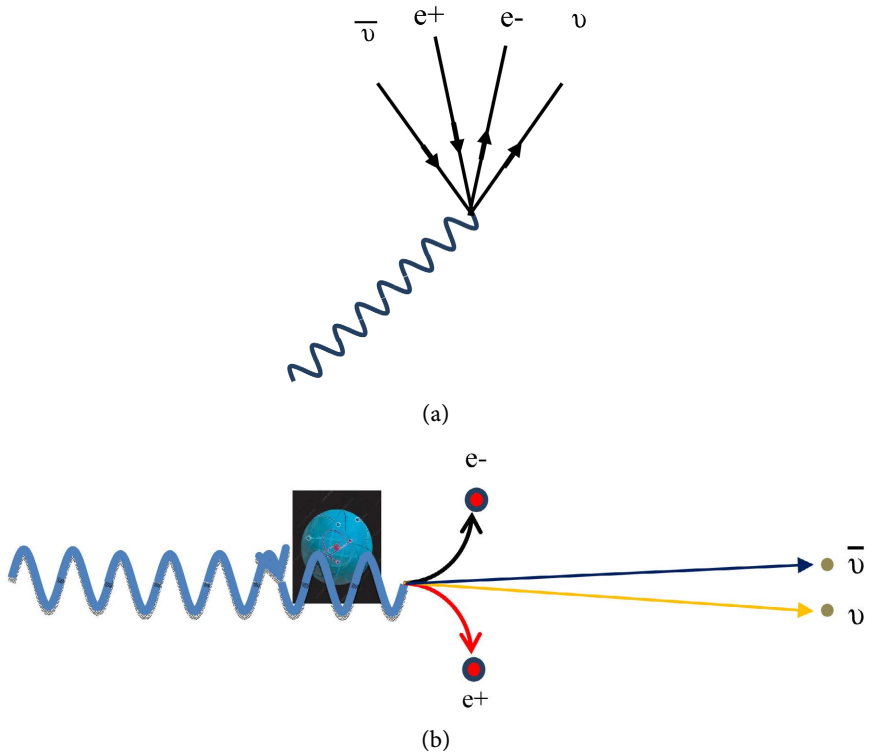

Figure 2. (a) Feynman diagram of electron-positron with neutrino-antineutrino pair production; (b) Illustration of proposed pair production process.

EGS5 [19]. Based on these improvements EGS5 calculations were used for the current study, with its geometry designed using CGVIEW, a program contained in the EGS5 code package, to describe a gamma ray beam passing through a Xenon detector (see **Figure 3**). The detector dimensions are $50 \times 50 \times 0.1$ cm inside a 75 cm-diameter air sphere surrounded by vacuum. The detector is made of a liquid Xenon slab 1 mm thick sandwiched between two 5 cm-thick slabs of air. The beam location is on the X axis at coordinates (−60 cm, 0, 0) directed in the positive X direction. Since pair production in EGS5 is dependent on gamma energy, calculation was executed for various gamma ray beam energies suitable for future experiments.

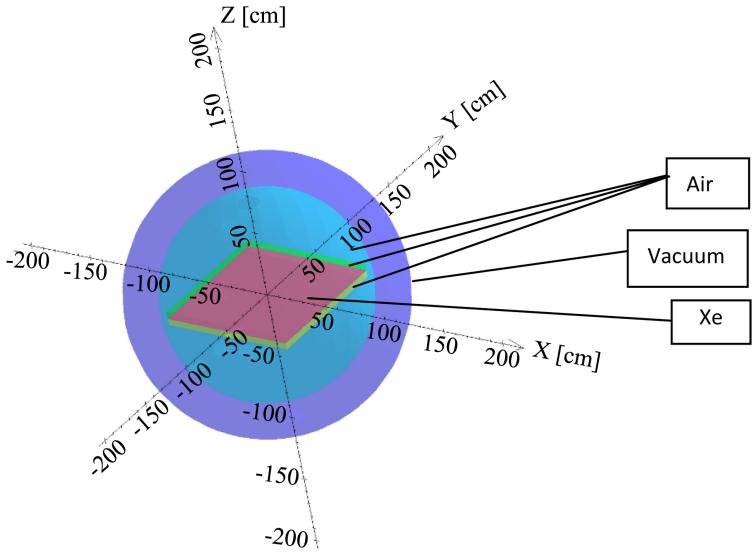

Figure 3. Simulation setup geometry and materials. The detector dimensions are 50 × 50 × 0.1 cm inside a 75 cm-diameter air sphere surrounded by vacuum.

In the "pair" subroutine of EGS5 ("egs5_pair.f") various energy ranges mark a difference in the way photon interaction is modeled. These energy edges are 2.1, 4.14, and 50 MeV; photons with energies within ranges between these energy levels are treated differently.

The energy carried out by the neutrino was simulated by making a change in two lines in the PAIR Subroutine, where the variables "theta" and "tteig" are calculated as follows:

$$\text{theta} = \text{RM}/(\text{eig}) \tag{1}$$

$$\text{tteig} = (\text{eig})/\text{RM} \quad \text{for} \quad \text{Eg} \geq 4.14 \ \text{MeV} \tag{2}$$

where,

RM = electron rest mass energy; and

eig = incident photon energy.

Theta is the polar angle of the outgoing electron, which correlates to the momentum conservation of the process. Therefore, the parameter "tteig" was calculated for the Motz-Olsen-Koch distribution that includes recoil energy and momentum [20]. The Motz-Olsen-Koch theoretical PP approach was implemented in EGS5 for gamma ray energy above 4.14 MeV.

In order to simulate the part of the photon energy that is carried out by the neutrino in the modified lines of the pair subroutine, for each gamma ray beam energy the variable "eig" was multiplied by 25% and 50%, meaning that the remainder of the energy was carried out by the neutrino-antineutrino.

3. Results and Discussion

We used a mono-energy gamma ray pencil beam source of 2.6 MeV, 4.5 MeV, 10 MeV, and 12 MeV to score the total deposited energy to the Xe detector for each case. Simulations were conducted using two different types of processes:

1) Original pair production process

2) Modified pair production process—a percentage of the momentum was transferred to the neutrino and the antineutrino, and was consequently reduced from the e−e+ pair.

We first simulated the system with its original condition, and then with modified pair production (PP), thereby showing that a percentage of momentum escaped with the neutrinos. Results of the absorption for 1E+07 histories are listed in Table 1 for each energy beam. A statistical error of about 0.15% was obtained for these results. The columns containing the scores for plain PP were compared to a case in which 50% of the momentum was carried by e+e−, and to a case in which 25% of the momentum was carried by e+e−. The neutrinos were not transported since the simulation does not have the capacity to track them, therefore were assumed to have escaped from the system without interactions.

Ratios presented in Table 1 reveal changes of less than 2% in detector response; hence, it would be very challenging to indicate whether or not neutrinos were created during the interaction.

In order to manifest resolution properties of the detector in the simulated liquid Xenon detector volume, two types of results were scored: a. spectral energy deposited in the Xenon detector; and b. the amount of energy transferred to produced positrons during a pair production occurrence. For each original run we changed the amount of momentum transferred to the e−e+ pair, a momentum deficit that was transferred to the hypothetical produced neutrino-antineutrino pair.

For photon energy below 4.14 MeV we simulated a gamma ray beam of 2.6 MeV, high enough above the PP energy threshold to produce a pair of e−e+. In Figure 4 spectrum ratios deposited in Xe by the 2.6 MeV beam are shown. Both calculated ratios introduce a relatively small difference of less than 3%, which would be barely detectable. Resulting events of energy transfer by produced positrons after pair production by 2.6 MeV beam are presented in Figure 5. In addition, n these counts, differences between each scenario events are hardly detectable along the detector depth.

In Figure 6, deposited spectra ratios of four incident photon energies in Xe are shown. The 50% ratios showed detectable anomalies below the photopeak energy. (For 5.0 MeV was not obtained.) The 25% ratios evinced a vast peak between 0.5 to 2.0 MeV, while for the 50% ratios that peak was barely detectable. These peaks' maxima varied from 4% to 10% depending on the beam's energy; therefore, we reckon that analysis of that region of the spectrum could reveal the proposed PP process. Even the anomalies around the photopeak are rather large, their detectability could be uncertain since multiple Compton scattering could interfere in that spectral region.

Events of energy transferred to produced positrons after pair production for 4.5 - 12 MeV beams are presented in Figure 7. The statistical error of these event values does not exceed 0.8%. The compared events for each model are presented in Figure 7; the changes are, for the most part, assumed as detectable in all cases.

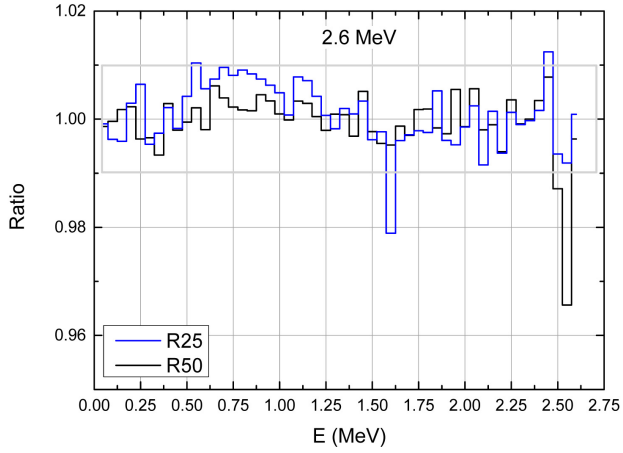

Figure 4. Spectral results of Xe response ratios of proposed to original pair production using 2.6 MeV photons. R25 - 25% of the total energy is transferred to e+e− while R50 - 50% of the total energy is transferred to e+e−.

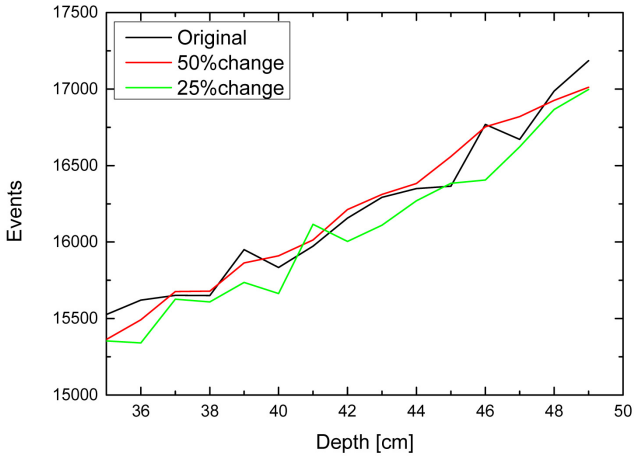

Figure 5. Photon beam of 2.6 MeV. Comparison of number of events resulting from produced positrons after pair production in the Xe. Original PP; 50% of the total energy transferred to e+e− while 25% of the total energy transferred to e+e−.

Table 1. Absorbed energy within the Xe detector as a result of 107 incident photons for these three cases: original PP process (without neutrino production); 50% of the PP energy transferred to electrons and positrons; and 25% of the PP energy transferred to electrons and positrons. Ratios obtained by normalizing the modified to the original process absorbed energy.

Ebeam (MeV)	Plain PP		50% Energy to e+e−		25% Energy to e+e−	
	Absorbed (MeV)	Ratio	Absorbed (MeV)	Ratio	Absorbed (MeV)	Ratio
2.6	11,679,138	1	11,678,047	0.9999	11,661,676	0.9985
4.5	16,874,336	1	16,827,416	0.9972	16,672,792	0.9881
10	26,739,942	1	26,638,851	0.9962	26,280,160	0.9828
12	29,802,801	1	29,703,683	0.9967	29,305,896	0.9833

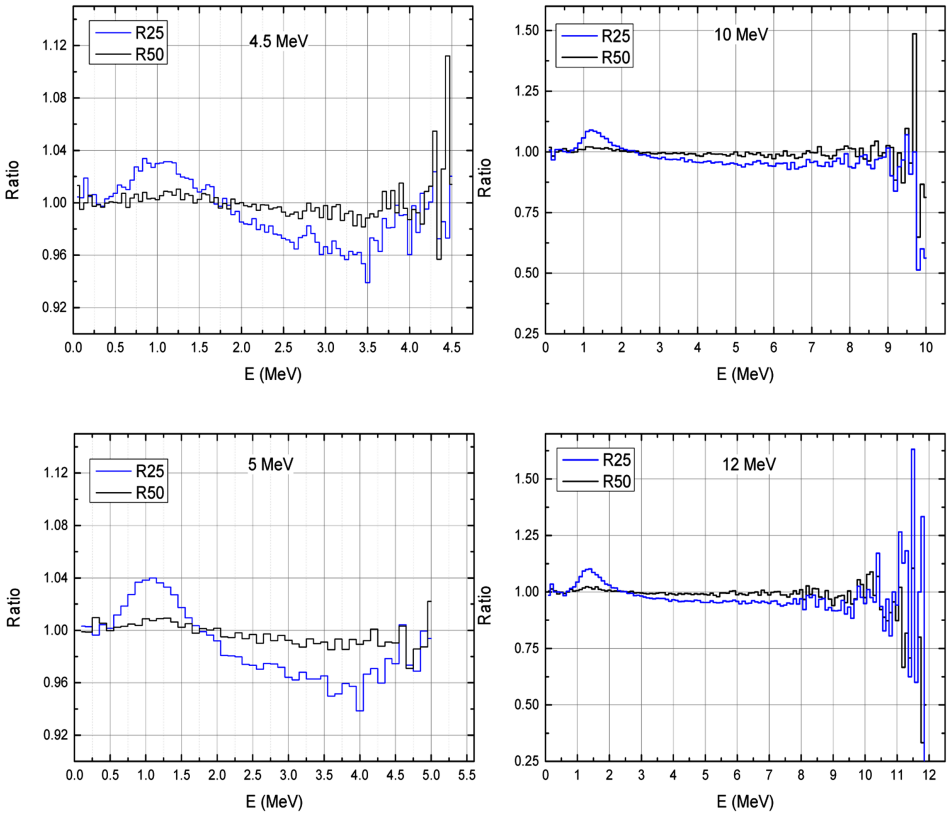

Figure 6. Spectral results of Xe response ratios of proposed to original pair production by photon beams of 4.5, 5, 10, and 12 MeV. R25 - 25% of the total energy is transferred to e+e−; while R50 - 50% of the total energy is transferred to e+e−.

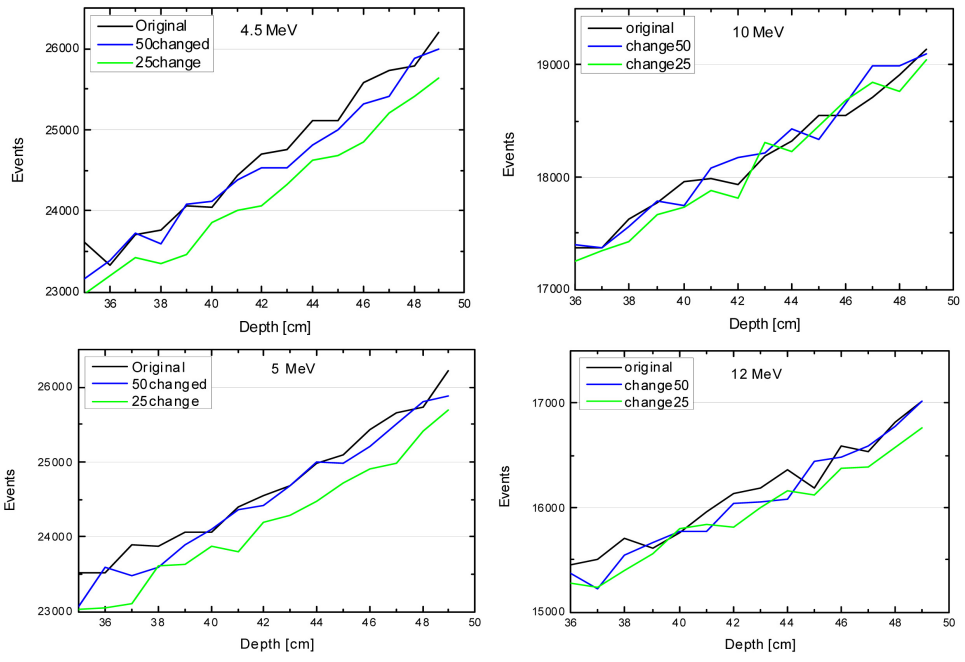

Figure 7. Photon beams of 4.5, 5, 10, and 12 MeV. Comparison of number of events from produced positrons after pair production. original PP; 50% of the total energy transferred to e+e−; while 25% of the total energy transferred to e+e−.

The new PP process presented in **Figure 2** that includes neutrinos, as might occur in reality, should also introduce a distribution of energy-momentum transfer to outgoing particles. Therefore, the percentage energy transfer to e+e− and to u, anti-u should be treated using a probability function. However, such process distribution rules are yet unknown, and require further exploration.

4. Conclusions

In the current study, the EGS5 Monte Carlo system was chosen to simulate a modified PP process that includes neutrino-antineutrino pair production. However, several other Monte Carlo codes also include PP interaction, electrons, and positrons transport. Comparing PP simulations using different Monte Carlo codes has been studied and reported [21], and their EGS5 results (marked as *EGS2*) plotted versus other much known codes. The same changes made for this study are applicable to these other codes (e.g., GEANT4), although factors extracted from published plot could spare one the effort.

The results in this paper indicate that a PP that includes neutrinos is detectable in cases in which the escaped neutrinos extract some fraction of the total momentum. The question is whether or not the PP process includes neutrino and antineutrino production, and it is recommended that this be experimentally studied.

Current estimates of neutrino flux in the galaxy contribute to small mass of the total estimated dark matter density to account for its entire amount. To date, the estimated total neutrino average number density is $n0\nu = 339.5\ cm^{-3}$ (The latest information on particle data is available on the web at: http://pdg.lbl.gov/pdg.html. This web page is maintained by the Particle Data Group at the Lawrence Berkeley laboratory). Gamma radiation from the sun at energies above 2.5 MeV is ~1 photons $cm^{-2}{\cdot}s^{-1}$ [22] that could produce an additional neutrino flux of ~20 $cm^{-2}{\cdot}s^{-1}$ neutrinos, at least. In the event that additional neutrino (antineutrino) flux is produced by gamma radiation from stars, as a result of the proposed PP process, the neutrino average number density would be higher by several orders of magnitude. Hence, a larger portion of the total estimated dark matter density may be contributed by neutrinos.

Conflicts of Interest

The authors declare no conflicts of interest regarding the publication of this paper.

References

[1] Brown, L.M. (1978) *Physics Today*, **31**, 23-28. https://doi.org/10.1063/1.2995181

[2] Bethe, H.A. and Peierls, R. (1934) *Nature*, **133**, 532. https://doi.org/10.1038/133532a0

[3] Dirac, P.A.M. (1928) *Proceedings of the Royal Society A*, **117**, 610-624. https://doi.org/10.1098/rspa.1928.0023

[4] Anderson, C.D. (1933) *Physical Review*, **43**, 491-494. https://doi.org/10.1103/PhysRev.43.491

[5] Hubbell, J.H. and Seltzer, S.M. (2004) *Nuclear Instruments and Methods in Physics Research B*, **213**, 1-9. https://doi.org/10.1016/S0168-583X(03)01524-6

[6] Hubbell, J.H. (2006) *Radiation Physics and Chemistry*, **75**, 614-623. https://doi.org/10.1016/j.radphyschem.2005.10.008

[7] Alkhateeb, S., Alshaery, A. and Aldosary, R. (2022) *Journal of Applied Mathematics and Physics*, **10**, 237-244. https://doi.org/10.4236/jamp.2022.102017

[8] Werner, C.J. (2017) LA-UR-17-29981: MCNP User's Manual, Code Version 6.2. https://mcnp.lanl.gov/pdf_files/la-ur-17-29981.pdf

[9] Allison, J., *et al.* (2016) *Nuclear Instruments and Methods in Physics Research A*, **835**, 186-225.

[10] Nelson, W.R., Hirayama, H. and Rogers, D.W.O. (1985) The EGS4 Code System. SLAC-Report-265.

[11] Peebles, P.J.E. and Ratra, B. (2003) *Reviews of Modern Physics*, **75**, 559-606. https://doi.org/10.1103/RevModPhys.75.559

[12] Frampton, P.H. (2018) Theory of Dark Matter. In: Fritzsch, H., Ed., *Cosmology, Gravitational Waves and Particles*, World Scientific, Singapore, 76-89. https://doi.org/10.1142/9789813231801_0008

[13] Bertone, G., Hooper, D. and Silk, J. (2005) *Physics Reports*, **405**, 279-390. https://doi.org/10.1016/j.physrep.2004.08.031

[14] Todorovic, Z. (2022) *Journal of High Energy Physics, Gravitation and Cosmology*, **8**, 593-622. https://doi.org/10.4236/jhepgc.2022.83042

[15] Kreisch, C.D., Cyr-Racine, F.-Y. and Dore, O. (2020) *Physical Review D*, **101**, Article ID: 123505. https://doi.org/10.1103/PhysRevD.101.123505

[16] Bertone, G. and Merritt, D. (2005) *Modern Physics Letters A*, **20**, 1021-1036. https://doi.org/10.1142/S0217732305017391

[17] Minamino, A. (XMASS Collaboration) (2010) *Nuclear Instruments and Methods in Physics Research—Section A*, **623**, 448. https://doi.org/10.1016/j.nima.2010.03.032

[18] Plante, G., Aprile, E., Budnik, R., Choi, B., Giboni, K.-L., Goetzke, L.W., Lang, R.F., Lim, K.E. and Melgarejo Fernandez, A.J. (2011) *Physical Review C*, **84**, Article ID: 045805. https://doi.org/10.1103/PhysRevC.84.045805

[19] Hirayama, H., *et al.* (2016) The EGS5 Code System. SLAC-R-730, KEK-2005-8, KEK-REPORT-2005-8, Version: January 13, 2016.

[20] Motz, J.W., Olsen, H.A. and Koch, H.W. (1969) *Reviews of Modern Physics*, **41**, 581-639. https://doi.org/10.1103/RevModPhys.41.581

[21] Gros, P. and Bernard, D. (2016) *Astroparticle Physics*, **88**, 60-67. https://doi.org/10.1016/j.astropartphys.2017.01.002

[22] Crannell, C.J., Crannell, H. and Ramaty, R. (1979) *The Astrophysical Journal*, **229**, 762-771. https://doi.org/10.1086/157012